Energy-Efficient Delay-Constrained Transmission and Sensing for Cognitive Radio Systems

Yuan Wu *Member IEEE*, Vincent K.N. Lau *Fellow IEEE*, Danny H.K. Tsang *Fellow IEEE*, Liping Qian *Member IEEE*

***Abstract*—In this work we study energy-efficient transmission for Cognitive Radio (CR) which opportunistically operates on Primary User's (PU's) channel through spectrum sensing. Spectrum sensing and compulsory idling (for incumbent protection) introduce energy-overheads for Secondary User's (SU's) operations, and thus an appropriate balance between energy consumption in data transmission and energy-overheads is required. We formulate this problem as a discrete-time Markov Decision Process (MDP) in which the SU aims at minimizing its average cost (including both energy consumption and delay cost) to finish a target traffic payload through an appropriate rate allocation. Based on *Certainty Equivalent Control*, we propose a low-complexity rate-adaptation policy that achieves comparable performance as the optimal policy. With the low-complexity policy, we quantify the impact of energy-overheads (including the power consumption for spectrum sensing and compulsory idling) on the SU transmission strategy. Specifically, the SU rate increases with the increase of energy-overheads, whose marginal impact, however, diminishes. Moreover, the marginal impact of energy-overheads is more significant for delay-insensitive traffic compared to that for delay-sensitive traffic. To mitigate the loss due to imperfect spectrum sensing, we quantify that the SU decreases (increases) its rate with a larger mis-detection probability (false alarm probability).**

I. Introduction

Cognitive radio, aiming at exploiting unused spectrum resource left by Primary User (PU), provide a promising path to relieve the current crisis of spectral congestion. Both exploitation of idle spectrum and incumbent protection for the primary system require special functionalities of CR, among which the spectrum sensing and compulsory idling[1] are the most distinctive from conventional wireless systems with licensed spectrum to use. The spectrum sensing and compulsory idling, however, consume additional system cost in terms of both time-overhead and energy-overhead. For example, the periodic spectrum sensing not only reduces the available transmission duration but also consumes static energy due to the RF circuits operation and baseband signal processing. Meanwhile, the compulsory idling also consumes energy to keep various parts of the RF circuits (such as the mixer, oscillators) operational[2]. Therefore, operational strategy of CR needs a careful design such that the Secondary User (SU) strikes an appropriate balance between the extra system overheads (e.g., energy consumption for spectrum sensing and compulsory idling) and the effective system cost for data transmission. Previous works studied this tradeoff by focusing on the SU spectrum sensing and access strategies [7]- [11], [13]–[15]. However, sensing and access strategies alone cannot fully capture the dynamic property when the SU faces a time-varying channel condition, thus losing of the aforementioned balance. In fact, the SU rate adaptation also plays a pivotal role in affecting this tradeoff. For example, the SU has to slow down its transmission to save transmit power under a deep fading channel (according to the principle of *opportunistic scheduling*). However, slowing down transmission not only causes degraded performance in delay but also incurs additional energy consumption for sensing and idling[3] in future slots. Therefore, the complex dynamics of the PU activities and the SU channel fluctuations as well as the additional burden of system-overheads necessitate an appropriate rate-adaptation strategy for CR to operate efficiently. This motivates our work.

There have been many works focusing on transmission strategies of CR. [16], [17] focused on maximizing system capacity under interference constraint for the PU system. [18], [19] focused on cooperative/distributed spectrum sharing among the SUs. However, rate adaptation as an approach for the SU energy-efficiency has seldom been considered.

This research is supported, in part, by the National Natural Science Foundation of China (Project No. 61101132), the Hong Kong Research Grants Council's GRF (Project No. 619911), the SFRI11EG17, the Zhejiang Provincial Key Science and Technology Innovative Team (Project No. 2010R50011), the Zhejiang Provincial Key Laboratory of Communication Networks and Applications, and the Zhejiang Provincial Natural Science Foundation (Project No. Y1101077).

Y. Wu is with College of Information Engineering, Zhejiang University of Technology, Hangzhou, 310023, China. He was with Department of Electronic and Computer Engineering, Hong Kong University of Science and Technology, Hong Kong (email: ecewuy@ust.hk). This work was partially carried out when Y. Wu was at the Hong Kong University of Science and Technology.

V.K.N. Lau is with Department of Electronic and Computer Engineering, Hong Kong University of Science and Technology, Hong Kong (email: eeknlau@ee.ust.hk).

D.H.K. Tsang is with Department of Electronic and Computer Engineering, Hong Kong University of Science and Technology, Hong Kong (email: eetsang@ece.ust.hk).

L.P. Qian is with College of Computer Science and Technology, Zhejiang University of Technology, 310023, China (email: lpqian@zjut.edu.cn).

[1]Compulsory idling refers to the situation that the SU has to stop its transmission and remain silent when the PU is occupying the licensed channel.

[2]Recent studies [1]–[3] have shown that appropriate management of power consumption in idling is critical to energy-saving of wireless networks. These results are consistent with manufacturers' datasheets [4] [5] that reveal a nonnegligible power consumption of transceiver chipsets in idling. Considering that the SU has to invoke compulsory idling frequently to avoid any harmful interference to the PU, an appropriate energy management that takes account of the SU energy consumption in idling is imperative to CR. This issue, however, has seldom been considered in the existing literatures.

[3]In the following we call the energy consumption for spectrum sensing and compulsory idling as energy-overheads.

This is the focus of our work. Different from previous works [7]- [11] [14] considering the time-overhead, we measure the system efficiency from the perspective of energy consumption. Specifically, we aim at investigating how the SU adapts its rate based on the PU activities, the SU channel fluctuations and its traffic state such that it strikes an optimal balance between the energy consumption for data transmission and the energy-overheads. Furthermore, we aim at investigating (i) how the SU energy-overheads influence its transmission strategy for traffic of different level of delay-sensitivity, and (ii) how the SU imperfect spectrum sensing influences its transmission strategy. To the best of our knowledge, the aforementioned two questions have not been well explored before.

Based on these considerations, we focus on the energy-efficient delay-constrained rate adaptation for the SU system. Our technical contributions are summarized below.

(i) *Optimal Policy and Low-Complexity Policy*: We first formulate the SU rate adaptation problem as a discrete-time Markov decision process where the SU aims at minimizing its average total cost (including both energy consumption and delay cost) to finish a target traffic payload. By viewing the problem as a stochastic shortest path problem, we derive the optimal rate-adaptation policy via the value iteration algorithm and analyze its structural properties in further. To reduce computational complexity, we propose a low-complexity rate-adaptation policy based on the *Certainty Equivalent Control (CEC) with approximation*.

(ii) *Performance Analysis based on the Low-Complexity Policy*: Based on our low-complexity policy, we quantify the impact of energy-overheads on the SU rate adaptation and the corresponding tradeoff between transmission delay and energy consumption. Our results indicate that the SU rate increases with the increase of energy-overheads whose marginal impacts, however, diminish. Moreover, the impacts of energy-overheads are more significant when the SU traffic is delay-insensitive.

(iii) *Impact of the Imperfect Spectrum Sensing*: We further consider the issue of imperfect SU spectrum sensing, and quantify the impact of mis-detection probability and false alarm probability on the SU rate adaptation. Our results indicate that to mitigate the loss due to the sensing error, the SU decreases (increases) its data rate with the increase of mis-detection probability (false alarm probability).

A. Related Works

In [7], the authors studied the tradeoff between the CR sensing accuracy and the effective throughput via tuning the spectrum sensing duration. In [8], the authors studied the tradeoff between the sensing cost and the missed spectrum opportunities by tuning the inter-sensing duration. Similar tradeoff was studied by the authors in [9] by considering the multi-channel scenario. However, most of these previous works [7]–[9] focused on the sensing strategy and used the time-overhead to measure the cost for spectrum sensing. The corresponding energy consumption was not included in their models, especially the energy consumption for compulsory idling. Different from [7]–[10] measuring the CR efficiency from the perspective of long-term statistics, another line of works exploited the time-varying system state to make the sensing and access decisions [12]- [14]. In [13], the authors studied the SU sensing and access policy to maximize the SU throughput during a battery lifetime. Different from [13], we focus on the SU rate-adaptation policy and consider both the delay sensitivity of SU traffic and the SU spectrum sensing error. None of these issues were addressed in [13]. In [14], the authors optimized the SU sensing duration and access policy to maximize the SU reward under the dynamics of PU activities. However, the SU channel fluctuation and the consequent SU rate adaptation were not considered in [14]. More importantly, none of these previous works [12]–[15] has quantified how the SU energy-overheads and sensing accuracy affect the operations of the SU. On the other hand, our work is also related to opportunistic scheduling policy under time-varying channel [21]–[23]. All these previous results in [21]–[23], however, are not directly applicable to CR due to the lack of considerations on the special functionalities of CR.

II. System Model and Problem Statement

In this section, we describe our system models, based on which we shall describe our problem statement. Table I includes the main notations we use in the rest of this work. For clarity, we use the upper case letters to denote the random variables, whose instances are denoted by the normal case letters.

We consider a CR system with a transmitter (SUTx) sending delay-sensitive data to a SU receiver (SURx). The SU system dynamically shares a common spectrum with a PU system using an overlaid approach. The PU system has priority in accessing the spectrum, and the SU system can transmit data only when the PU system is idle (as illustrated in the top subfigure in Fig. 1). The SU system dynamically learns the intermittent activities of the PU system using the periodic spectrum sensing. Specifically, in the PU system with slotted structure (of length T), the SU first detects the PU's activity and estimates the channel condition between the SUTx and the SURx during the estimation sub-slot with duration t_{se}. If the sensing result indicates that the PU is idle, then the SUTx delivers the payload to the SURx with rate r_k in the payload sub-slot with duration $t_{tr} = T - t_{se}$. Otherwise, the SUTx remains idle during the current payload sub-slot. We shall elaborate the PU activity model, the SU energy consumption model, the rate-adaptation policy and the problem statement in the following subsections, respectively.

A. The PU Activity Model

Suppose that time is divided into slots with equal size T and indexed by $k = 1, 2, ...$ Let $S_k \in \mathcal{S} = \{0, 1\}$ denote the PU activity state at slot k. $S_k = 1$ ($S_k = 0$) denotes the PU is idle (busy), i.e., its channel is available (unavailable) for the SU to use. We have the following assumption on the PU activity process $\{S_k\}$.

Assumption 1: (PU Activity Model) The PU activity process $\{S_k\}$ is a time-homogenous Markov chain with the transition probability given by $\theta_{ss'} = \Pr\{S_{k+1} = s' | S_k = s\}, s, s' \in$

TABLE I
NOTATION LIST

Symbol	Definition
$S_k \in \{0,1\}$	the PU state at slot k
$\widetilde{S}_k \in \{0,1\}$	the SU sensing result at slot k
$G_k \in \mathcal{G}$	the SU channel power gain at slot k
$\Theta_0(\Theta_1)$	the stationary probability that the PU state is busy (idle)
$\eta_g, \forall g \in \mathcal{G}$	the stationary probability that the SU channel gain is g
ϕ_{se}, ϕ_{id}	the SU power consumption for sensing and compulsory idling
T	the slot length
t_{se}, t_{tr}	the durations for spectrum sensing and transmission
$V^{\max}$	the SU maximum payload
λ	the SU marginal delay cost
r_k	the SU rate allocation at slot k
$\Phi_{tx}(r_k, G_k)$	the SU transmission power to guarantee its rate r_k at channel gain G_k

$\mathcal{S}$. Furthermore, this Markov process is ergodic with $\Theta_0 = \Pr\{S_k = 0\}$ denoting the stationary distribution that PU is busy, and $\Theta_1 = 1 - \Theta_0$ denoting the stationary distribution that the PU is idle. □

B. The SU Channel Fluctuation and Energy Consumption Model

Let G_k denote the channel power gain from the SUTx to the SURx at slot k. Considering a short-term memory in fading process, we have the following assumption on the SU channel fading process $\{G_k\}$.

Assumption 2: (SU Channel Fluctuation Model) The SU channel fading process $\{G_k\}$ is a time-homogeneous Finite State Markov Chain (FSMC) with the one-step transition probability given by $\eta_{gg'} = \Pr\{G_{k+1} = g' | G_k = g\}, g, g' \in \mathcal{G}$. $\mathcal{G}$ is a finite set of discretized channel gains. Furthermore, we assume that the Markov process is ergodic with $\eta_g = \Pr\{G_k = g\}$ denoting the stationary distribution that the SU channel gain is in state $g \in \mathcal{G}$.□

The FSMC has been widely used to model the block fading channel for packet-level communication with block length sufficiently long [13], [14], [22]–[24]. In [26] the slowly-varying Rayleigh fading channel was modeled as a FSMC through partitioning the received signal to noise ratio (SNR) into a finite number of states. The assumption of first-order Markovian was further validated in [27] with its accuracy demonstrated. Using the similar equal-probability partition approach as [22] [26], we model the slowly-varying Rayleigh fading channel as a FSMC to facilitate our following numerical illustrations[4].

Meanwhile, we assume that the SUTx and SURx can achieve an accurate channel estimation by using the robust pilot-aided technique [25], i.e., we have the following assumption.

Assumption 3: (Perfect Channel Estimation) The SUTx and SURx obtain perfect knowledge of G_k at the beginning of slot k. □

[4]It is also noted that the Jakes' model has been widely used for Rayleigh fading process. Since it has been shown experimentally that the FSMC can match the measured fading channel process quite accurately [26]–[29], and in practice physical layer can only support a discrete set of rate allocations for transmission, we adopt the FSMC in both our analysis and simulation to strike a balance between analytical tractability and practicality.

Based on assumptions 1-3, the SU energy consumption model is elaborated as follows. The top subfigure in Figure 1 presents a detailed example. At the beginning of each slot k, the SU spends duration t_{se} for both sensing the PU activity and estimating its own channel gain. Hence, the energy consumption for sensing is given by $t_{se}\phi_{se}$, where ϕ_{se} is the SU sensing power. Note that t_{se} is a system parameter of the SU system and is determined according to the requirement on sensing accuracy (we first consider the perfect spectrum sensing. The issue of imperfect spectrum sensing will be addressed in Section V). We shall illustrate the other parts of energy consumption according to the following two cases.

Case 1: If $S_k = 1$, then the SU carries out data transmission within the rest duration $t_{tr} = T - t_{se}$. Specifically, the received signal Y_k by the SURx can be expressed as $Y_k = S_k(G_k X_k + Z_k)$, where X_k is the transmitted symbol at slot k, and Z_k is the AWGN channel noise with normalized unit variance. Therefore, the data rate of SU can be expressed as $r_k = S_k \log_2(1 + \xi \Phi_k G_k)$, where ξ is some constant, and Φ_k denotes the SU transmit power. Note that the data rate expression can represent both uncoded and coded scenarios. For example, when $\xi = \frac{c_2}{\ln(c_1/\text{BER})}$ (for some constants c_1, c_2), this corresponds to the uncoded MQAM scenario, and BER denotes a target bit error rate requirement at SURx. On the other hand, when $\xi = 1$, this corresponds to the scenario of powerful error correction codes (e.g., LDPC), and the data rate becomes the instantaneous mutual information. Without loss of generality, we set $\xi = 1$ in the rest of the paper but the results can be applied to the uncoded case as well [22]. Since the SU transmission power depends on the data rate as well as the channel gain G_k, we denote it by $\Phi_{tx}(r_k, G_k) = \frac{1}{G_k}(2^{r_k} - 1)$, and the SU energy consumption for transmission in this case is given by $\Phi_{tx}(r_k, G_k)t_{tr}$ at slot k.

Case 2: If $S_k = 0$, then the SU has to keep idle within the rest duration t_{tr}, and its energy consumption for idling is $\phi_{id}t_{tr}$, where ϕ_{id} is the SU power consumption during idling. Notice that according to the datasheets [4], [5], the SU still consumes non-negligible power to keep various parts of the RF circuits operational even it is in idling. This power consumption in idling has been ignored in most existing literatures on CR. However, as we shall illustrate, this power consumption also has a non-negligible impact on the SU rate adaptation.

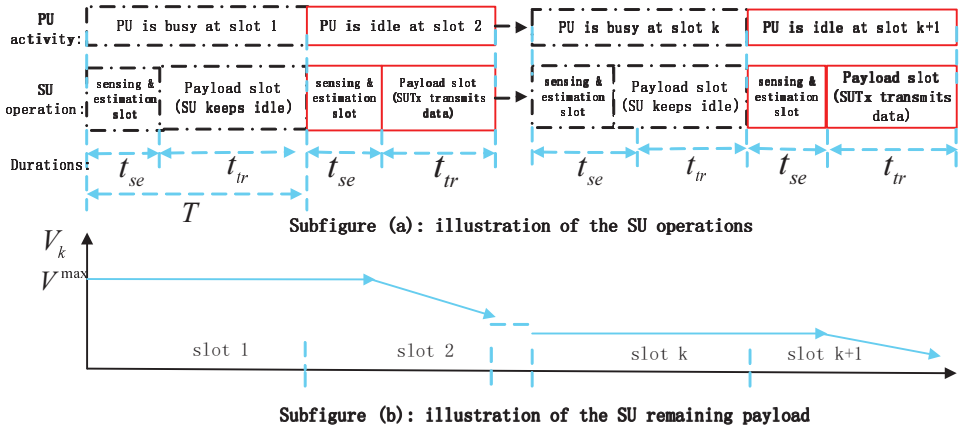

Fig. 1. Subfigure (a): Illustration of the SU operations. If $S_k = 0$, the SU will keep idle (marked with the dash-dot rectangle) after spectrum sensing. In this situation, the SU consumes sensing energy $\phi_{se}t_{se}$ and idling energy $\phi_{id}t_{tr}$ at slot k. If $S_k = 1$, the SU will carry out transmission with rate r_k (marked with the solid rectangle). In this situation, the SU consumes sensing energy $\phi_{se}t_{se}$ and transmission energy $\Phi_{tx}(r_k, G_l)t_{tr}$ at slot k. The whole process continues until the SU target payload is finished. Subfigure (b): Illustration of the dynamics of the SU remaining payload to be delivered.

As a result, the total energy consumption of the SU system in the k-th slot is summarized as follows

$$c_E(S_k, G_k, V_k, r_k) = \begin{cases} \phi_{se}t_{se} + \phi_{id}t_{tr}, \text{ if } S_k = 0, V_k > 0, \\ \phi_{se}t_{se} + \Phi_{tx}(r_k, G_k)t_{tr} + I_{[r_k=0]}\phi_{id}t_{tr}, \text{ if } S_k = 1, V_k > 0, \\ 0, \text{ otherwise}, \end{cases}$$

where V_k denotes the SU remaining payload to be delivered from slot k, and $I_{[.]}$ is the indicator function with $I_{[r_k=0]}\phi_{id}t_{tr}$ representing that the SU consumes energy $\phi_{id}t_{tr}$ for being idle. The last case corresponds to the situation that the SU finishes all the payload bits already.

C. The SU Delay Cost and Problem Statement

The SUTx is assumed to have a target payload of $V^{\max}$ bits at the beginning of the 1st slot ($k = 1$). The evolution of $\{V_k\}$ is given by: $V_{k+1} = \max\{V_k - t_{tr}r_k, 0\}, k \geq 1$ (as shown in the bottom subfigure in Fig. 1). We impose a delay cost λ at every slot as long as there are leftover bits in the buffer of the SUTx. The above delay cost model reasonably characterizes the delay penalty in a system with deterministic arrivals such as VoIP in which $V^{\max}$ represents the packet size of each talkspurt [32]. In this case, the delay is defined as the number of slots taken by the SU to finish its target payload of size $V^{\max}$. In particular, the delay cost λ represents the *delay-sensitivity* of the SU traffic. By varying λ, we characterize the Pareto optimal boundary of the SU traffic delay versus the SU energy consumption (as illustrated in the left subfigure in Fig. 5). Furthermore, we quantify the impact of SU energy-overhead on its optimal rate adaption policy under different levels of delay-sensitivity.

Considering both the delay and energy consumption costs, the instantaneous total SU cost at slot k is given by

$$c(S_k, G_k, V_k, r_k) = c_E(S_k, G_k, V_k, r_k) + \lambda I_{[V_k>0]}. \quad (1)$$

In this paper, we are interested to determine the optimal rate adaptation strategy so as to minimize the average total cost to finish the delivery of the SU target payload. Mathematically, the problem is given by

(P1):

$$\min_{\{r_k\}} \lim_{K\to\infty} \mathbb{E}\Big\{ \sum_{k=1}^{K} c(S_k, G_k, V_k, r_k) | (S_1, G_1, V_1 = V^{\max}) \Big\}, \quad (2)$$

where S_1 and G_1 represent the initial PU state and the SU channel condition, respectively. Since both S_k and $G_k, k > 1$ can only be observed at the beginning of the k-th slot, problem (P1) is a *total cost minimization problem over an infinite horizon* [36]. In particular, the SU cost in (1) can also be understood from a constrained optimization perspective. λ can be considered as the Lagrangian multiplier of the average delay constraint $\lim_{K\to\infty} \mathbb{E}\big\{ \sum_{k=1}^{K} I_{[V_k>0]} | (S_1, G_1, V_1 = V^{\max}) \big\} \leq \overline{D}$, which requires the SU to finish delivery of the target payload of size $V^{\max}$ within $\overline{D}$ slots on average. A more detailed description will be made in remark 1 in section III.

III. Markov Decision Process and The Optimal Policy

In this section, we shall illustrate that problem (P1) can be expressed as a *stochastic shortest path Markov Decision Process (MDP)* problem. Based on that, we shall show the existence of optimal rate-adaptation policy which is stationary and deterministic. We shall further discuss the impact of SU energy-overheads on its optimal policy.

A. Markov Decision Process

We first present our problem (P1) as an MDP problem by specifying the system state, action space, transition kernel and the per-stage cost as follows.

(i) System State: the system at each slot k can be characterized by a three-tuple $X_k = (S_k, G_k, V_k) \in \mathcal{S} \times \mathcal{G} \times \mathcal{V}$, where V_k denotes the remaining payload to be finished. $\mathcal{S}$ and $\mathcal{G}$ are the underlying spaces for the PU activity (defined in assumption 1) and the SU channel condition (defined in

assumption 2), respectively. $\mathcal{V} = \{0, 1, ..., V^{\max}\}$ is the state space for the SU remaining payload. For clarity, we drop the time index and use (s, g, v) to denote the current system state.

(ii) Action Space and Rate-Adaptation Policy: Given the system state (s, g, v), the SU determines its rate $r \in \mathbb{R}(s)$ according to a rate-adaptation policy π defined in the following definition 1. Specifically, $\mathbb{R}(s)$ is the SU action space when the PU state is s. $\mathbb{R}(0) = \{0\}$ since the SU is not allowed to transmit when the PU is busy. Meanwhile, $\mathbb{R}(1) = \{0, \Delta, 2\Delta, ..., L^{\max}\Delta\}$, where Δ denotes the step-size for the SU rate adaptation, and $L^{\max}\Delta$ is the maximum transmission rate of the SUTx. Specifically, we set $\Delta = \frac{1}{t_{tr}}$, which is equivalent to delivering one unit of payload within a payload sub-slot (as shown in Fig. 1).

Definition 1: (Rate-Adaptation Policy) A rate-adaptation policy π_k at slot k denotes a mapping from the system state $(s, g, v) \in \mathcal{S} \times \mathcal{G} \times \mathcal{V}$ to a probability distribution $\Pr\{r|(s, g, v)\}$ on the SU rate-adaptation space $\mathbb{R}(s)$. Furthermore, let $\Omega = \{\pi_1, \pi_2....\pi_k, ...\}$ denote the sequence of rate adaptation policies at different slots. □

(iii) Transition Kernel: Let $\Pr\{r|(s, g, v)\}$ be the conditional probability of a rate allocation r given the state (s, g, v) (this setup embraces the randomized policy as well). Given the system state (s, g, v), the one-step transition probability to the next system state (s', g', v') is given by

$$\Pr\{(s', g', v')|(s, g, v)\} = \theta_{ss'}\eta_{gg'}\Pr\{r|(s, g, v)\}I_{[v'=v-rt_{tr}]}, \text{ when } v > 0. \quad (3)$$

We assign $\Pr\{(s', g', 0)|(s, g, v)\} = \theta_{ss'}\eta_{gg'}$ when $v = 0$.

(iv) Per-stage Cost: Based on the transition kernel and the cost formula (1), the SU per-stage cost is given by $\sum_{r\in\mathbb{R}(s)} c(s, g, v, r)\Pr\{r|(s, g, v)\}$.

In particular, there exists a special group of states (called *terminal states*), i.e., $(s, g, 0), \forall s, g$, which represent that the SU finishes its target payload already and no more per-stage cost will be incurred afterwards. Since the SU eventually has to finish its target payload and enters the terminal state (otherwise, its total cost will be infinite), problem (P1) is equivalent to a stochastic shortest path MDP as follows

$$\textbf{(P2):} \ [\pi_1^*, ..., \pi_k^*, ...\pi_{\hat{K}}^*] = \arg\min_{\Omega} \mathbb{E}\Big\{\sum_{k=1}^{\hat{K}} c(S_k, G_k, V_k, r_k)|(S_1, G_1, V^{\max})\Big\}, \quad (4)$$

where $\hat{K} = \min\{k|V_k = 0\}$ denotes the slot that the SU finishes its target payload and enters the terminal state. Note that $\hat{K}$ is a random variable because of the randomness of the PU activity and the SU channel fluctuation. In particular, the rate-adaptation policy affects the average cost via both the per-slot cost and the underlying probability measure. We first have the following theorem regarding the optimality of stationary deterministic policy with respect to problem (P2).

Theorem *1: (Optimality of Stationary Deterministic Policy)* Problem (P2) admits an optimal policy which is deterministic and stationary[5]. □

[5]The deterministic policy means that the chosen action is a deterministic (instead of randomized) mapping from the system state to the action space. Meanwhile, the stationary policy means that the policy is time-homogeneous.

The proof is given in the appendix. Based on theorem 1, we focus on the stationary and deterministic policy $\Omega = \underbrace{\{\pi, ...\pi, ..\pi\}}_{\hat{K}}$ in the rest of the paper, and we can simply use policy π to represent Ω. Specifically, let $\pi^* = r^*(s, g, v), \forall(s, g, v) \in \mathcal{S}\times\mathcal{G}\times\mathcal{V}$ denote the optimal stationary policy (now we do not have to include the time index for the optimal policy). Meanwhile, let $J(s, g, v)$ denote the optimal average total cost to finish payload v starting from the system state (s, g, v). $J(s, g, v)$ is known as the *optimal cost-to-go* from the perspective of Dynamic Programming (DP). The optimal policy satisfies the *Bellman's equation* as follows

$$J(s, g, v) = c(s, g, v, r^*(s, g, v)) + \mathbb{E}_{s',g'}[J(s', g', v - t_{tr}r^*(s, g, v))|(s, g)], \forall(s, g, v). \quad (5)$$

Remark 1: (Marginal Delay Cost as the Lagrangian Multiplier) The marginal delay cost λ can be considered as the Lagrangian Multiplier (LM) for the following constraint

$$\lim_{K\to\infty} \mathbb{E}\Big\{\sum_{k=1}^{K} I_{[V_k>0]}|(S_1, G_1, V_1 = V^{\max})\Big\} \le \overline{D}, \quad (6)$$

where $\overline{D}$ is the average delay requirement to finish the SU target payload. Consider the following problem

$$\textbf{(P3):} \ \min_{\pi} \lim_{K\to\infty} \mathbb{E}\Big\{\sum_{k=1}^{K} c_E(S_k, G_k, V_k, r_k)|(S_1, G_1, V_1 = V^{\max})\Big\}, \quad \text{subject to: } (6).$$

Note that the stochastic shortest path problem (P2) with the delay cost λ is equivalent to the Lagrangian function of problem (P3) after incorporating the delay constraint (6) into the objective function. The following lemma established the zero duality gap between problems (P2) and (P3). The proof is given in the appendix. □

Lemma *1: (Zero Duality Gap)* Suppose that problem (P3) is feasible. Let π^* and λ be the optimal policy and the delay cost for problem (P2). If the delay constraint (6) is strictly binding with policy π^*, then policy π^* is also optimal for problem (P3) with λ serving as the corresponding Lagrangian multiplier.□

Note that if $\overline{D}$ is sufficiently large such that condition (6) is slack at the optimum of problem (P3), then the value of $\lambda = 0$. Otherwise, the value of λ can be determined by using the bisection method in order to reach the specified average delay $\overline{D}$, i.e., $\lambda = \inf\{\lambda'|D(\lambda') \le \overline{D}\}$ where $D(\lambda')$ is a function measuring the average delay with the delay cost λ' [6]. In the following, we consider that the traffic delay cost λ is predetermined to reach a certain average delay requirement. As described before, introducing a fixed λ guarantees the existence of an optimal policy which is both deterministic and stationary (according to Theorem 1), thus facilitating our following performance analysis. Moreover, since λ represents

[6]On the other hand, if there does not exist a λ such that the SU average delay to finish $V^{\max}$ is equal to $\overline{D}$, then the optimal policy for (P3) takes the form of a randomized mixture of two deterministic policies. Both of these two deterministic policies can be obtained through solving the Lagrangian parameterized problem (P2) with two different values of λ [23] [24] [31].

the delay sensitivity of the SU traffic, using a fixed λ facilitates our following evaluation on how the delay sensitivity of SU traffic influences the optimal SU rate-adaptation policy under different energy-overheads[7].

B. Value Iteration and The Optimal Policy

The optimal policy for problem (P2) can be derived through the value iteration algorithm, in which $J(s,g,v)$ is iteratively determined by

$$J(s,g,v) = \min_{z\in\mathbb{R}(s)} Q(s,g,v,z) = \min_{z\in\mathbb{R}(s)} \big\{c(s,g,v,z) + \mathbb{E}_{s',g'}[J(s',g',v-t_{tr}z)|(s,g)]\big\}. \quad (7)$$

We initialize $J(s,g,0)=0$ for all terminal states. $Q(s,g,v,r)$ represents the Q-factor associated with the rate allocation r at the system state (s,g,v) [36]. Since $r=0$ is the only feasible rate allocation when the PU is busy (i.e., $s=0$), the corresponding value iteration can be simplified as

$$J(0,g,v) = Q(0,g,v,0) = \big(t_{se}\phi_{se} + t_{tr}\phi_{id} + \lambda\big) + \mathbb{E}_{s',g'}[J(s',g',v)|(s,g)]. \quad (8)$$

The value iterations (7) and (8) are guaranteed to converge to the optimal cost $J(s,g,v)$ from arbitrary initialization [36]. After convergence, the optimal rate allocation policy is determined by $r^*(s,g,v) = \arg\min_{z\in\mathbb{R}(s)} Q(s,g,v,z)$ when $s=1$, and $r^*(s,g,v)=0$, otherwise.

C. Impact of Sensing Overheads on the Optimal Policy

We characterize the impact of SU energy-overheads on its optimal rate-adaptation policy in the following theorem. The proof is given in the appendix.

Theorem *2: (Monotonicity Property of the Optimal Policy)* The optimal cost $J(s,g,v)$ is increasing in the power consumption for spectrum sensing (i.e., ϕ_{se}) and the power consumption for compulsory idling (i.e., ϕ_{id}). Meanwhile, the optimal rate-adaptation $r^*(1,g,v)$ is nondecreasing in ϕ_{se} and ϕ_{id} when the sensing result is idle. □

Remark 2: (Explanation of the Monotonicity Property of Optimal Policy) The property that $r^*(1,g,v)$ is nondecreasing in ϕ_{se} and ϕ_{tr} is consistent with the intuition. A larger sensing power ϕ_{se} (or idling power ϕ_{id}) will introduce a larger energy-overhead. Therefore, the SU shortens its duration in data transmission (i.e., by transmitting faster) to reduce its energy consumption in sensing and idling. Figure 2 verifies the impact of ϕ_{se} and ϕ_{id} on the SU rate adaptation. Specifically, the comparison between the two top-subfigures indicates that the SU increases its rate with a larger sensing power ϕ_{se}. Meanwhile, the comparison between the two bottom-subfigures indicates that the SU increases its rate with a larger idling power ϕ_{id}. In the next section, we further quantify the impact of ϕ_{se} and ϕ_{tr} by deriving a low-complexity policy. □

Remark 3: (Complexity of the Optimal Solution) Deriving the optimal policy via the value iteration (which corresponds to solving a fixed point of equations (7) and (8) with $2|\mathcal{G}||\mathcal{V}|(L^{\max}+1)$ unknown variables) requires a high computational complexity. For example, in each round of iteration, the number of operation of multiplication is in order of $\mathcal{O}\big(2(L^{\max}+2)|\mathcal{G}||\mathcal{V}|\big)$, where $|\mathcal{G}|$ and $|\mathcal{V}|$ denote the cardinality of the feasible space of the SU channel condition and the cardinality of the feasible space of the SU remaining payload, respectively. This usually prohibits application of the optimal policy in real scenario. Therefore, we derive a low-complexity policy for the SU rate adaptation based on the principle of *CEC with approximation* in the next section. □

[7]In particular, another choice is to use a delay cost function which is time-increasing, e.g. $k\lambda$, to represent the delay-sensitive traffic. We intend to leave this choice as our future work.

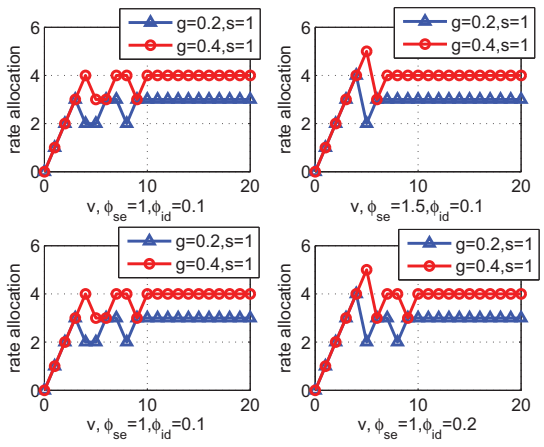

Fig. 2. The impact of sensing power and idling power on the optimal SU rate adaptation. For clear illustration of the optimal policy, we consider a representative two-state channel condition $\mathcal{G}=\{0.2,0.4\}$ with the one-step transition probabilities between the two different channel states as 0.55 (from $g=0.2$ to $g=0.4$) and 0.35 (from $g=0.4$ to $g=0.2$). The two top-subfigures show the optimal rate allocation profiles under the spectrum sensing power $\phi_{se}=1$ and $\phi_{se}=1.5$, respectively. The two bottom-subfigures show the optimal rate allocation profiles under the idling power $\phi_{id}=0.1$ and $\phi_{id}=0.2$, respectively.

IV. The Low-Complexity Rate Adaption Policy

In this section, we shall derive a low-complexity policy for the SU rate adaptation. Based on the low-complexity policy, we quantify the impact of energy-overheads on the SU rate adaptation and show the corresponding tradeoff between the average energy consumption and the average traffic delay (under different SU energy-overheads).

A. Overview of the Certainty Equivalent Control with Approximation

We design a low-complexity policy for the SU rate adaptation based on the CEC with approximation. The CEC is an approach for suboptimal control in which the control decision at each stage is optimized by fixing unknown quantities in future at their "typical" values. For example, consider a total cost minimization problem over a finite horizon with length N [36]. The rule of CEC works as the following two steps.
Step (i) At each stage k and system state x_k, find the control sequence $\{\overline{u}_i\}_{i=k,k+1,\ldots,N-1}$ that solves the following deterministic problem (specifically, $c_k(x_k,u_k,w_k)$ represents the per-stage cost, which depends on the system state x_k, the

chosen action u_k, and the random system disturbance w_k)

$$\min_{\{u_i\}_{i=k,k+1,\ldots,N-1}} c_N(x_N) + \sum_{i=k}^{N-1} c_i\big(x_i, u_i, \overline{w}_i(x_i, u_i)\big), \quad (9)$$

where $x_{i+1} = f_i(x_i, u_i, \overline{w}_i(x_i, u_i)), i = k, k+1, ..., N-1$ specifies the transition of the system state, and $\overline{w}_i(x_i, u_i)$ denotes the typical value of the random disturbance at stage i with state-action pair (x_i, u_i).

Step (ii) Apply $\overline{u}_k$ (i.e., the first element of the derived optimal control sequence) at stage k. Then go back to Step (i) to determine the action at the next stage.

However, since the actions at different stages are correlated through the transitions of the system states, evaluating $\sum_{i=k}^{N-1} c_i(x_i, u_i, \overline{w}_i(x_i, u_i))$ in each round of iteration (including aforementioned Step (i) and Step (ii)) still requires considerable computational complexity. One way to reduce this computational complexity is to approximate the aggregate cost function in the future stages. Based on this rationale, the control decision at each stage aims at optimizing the sum of the current stage cost and the *approximated aggregate cost* in future stages. Let $H_{k+1}(x_{k+1})$ denote the approximated aggregate cost function in the future stages starting from state x_{k+1}. Thus, the approximated problem for problem (9) is given by

$$\min_{u_k} c_k(x_k, u_k, \overline{w}_k(x_x, u_k)) + H_{k+1}(f_k(x_k, u_k, \overline{w}_k(x_k, u_k))), \quad (10)$$

with the assumption that the disturbances in the future slots are fixed at their typical values $\overline{w}_i(x_i, u_i), i = k, k+1, ...N-1$.

Policy based on the CEC is proved to be optimal for the linear-quadratic problem, and moreover, the CEC with approximation still performs well for other problems and yields near-optimal policies [36]. Essentially, the CEC (with approximation) follows the rationale behind the Bellman's equations, i.e., decision at each stage aims at achieving a good balance between the current stage cost and the (approximated) aggregate cost in the future stages. By exploiting the statistical information on the future states, the policy based on the CEC with approximation can achieve comparable performance as the optimal policy. The details on the approach of CEC with approximation can be referred to [36].

B. The Low-Complexity Policy via the CEC with Approximation

We derive the low complexity rate-adaptation policy by using the CEC with approximation. Problem (P2) is first approximated by a two-stage optimization problem which includes (Stage-I) in (11) and (Stage-II) in (12). Specifically, given the system state (S_k, G_k, V_k) at slot k and the SU rate allocation r_k, in (Stage-II) we first approximate the optimal aggregate cost $H(.)$ (to finish the remaining traffic volume) in the future slots by fixing the system uncertainties at their typical values. Then, in (Stage-I), by using the approximated $H(.)$, we determine r_k such that the SU achieves the best tradeoff between the cost in the current slot k and the approximated aggregate cost in the future slots. Figure 3 illustrates the interaction between these two stages. Our design of this two-stage optimization problem essentially follows the principle of CEC with approximation. The details are elaborated as follows.

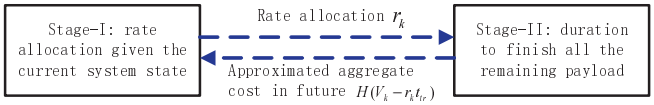

Fig. 3. Illustration of the two-stage problem and the interaction between problem (Stage-I) and problem (Stage-II).

The first stage problem (when $S_k = 1$) is given by

$$\textbf{(Stage-I):} \ \min_{r_k} t_{se}\phi_{se} + t_{tr}(2^{r_k} - 1)\frac{1}{G_k} + I_{[r_k=0]}\phi_{id}t_{tr} + \lambda I_{[V_k>0]} + H(V_k - r_k t_{tr}). \quad (11)$$

$t_{se}\phi_{se} + t_{tr}(2^{r_k} - 1)\frac{1}{G_k} + I_{[r_k=0]}\phi_{id}t_{tr}$ denotes the SU energy consumption in the current slot. Meanwhile, $V_k - t_{tr}r_k$ denotes the remaining payload to be finished after slot k, and the corresponding function $H(V_k - t_{tr}r_k)$ represents the expected cost (including both the cost for energy consumption and the delay cost) to finish $V_k - t_{tr}r_k$ in the future slots. Specifically, the value of $H(V_k - t_{tr}r_k)$ is determined by the second stage problem as follows

$$\textbf{(Stage-II):} \ H(V_k - t_{tr}r_k) = \min_{q} qt_{tr}(2^{\frac{V_k - r_k t_{tr}}{qt_{tr}}} - 1)\frac{1}{\overline{g}} + \frac{q}{\Theta_1}\phi_{se}t_{se} + (\frac{q}{\Theta_1} - q)\phi_{id}t_{tr} + \lambda\frac{q}{\Theta_1}. \quad (12)$$

In (12), the SU calculates $H(V_k - t_{tr}r_k)$ by determining q, which can be interpreted as the number of idle slots for the SU data transmission. By fixing its channel gain at the average value $\overline{g} = \sum_{g\in\mathcal{G}} g\eta_g$, the SU approximates its energy consumption (for effective data transmission) by $qt_{tr}(2^{\frac{V_k - r_k t_{tr}}{qt_{tr}}} - 1)\frac{1}{\overline{g}}$ in order to finish its remaining payload. Meanwhile, in order to find q idle slots, on average the SU has to consume the energy-overheads equal to $\frac{q}{\Theta_1}\phi_{se}t_{se} + (\frac{q}{\Theta_1} - q)\phi_{id}t_{tr}$ for spectrum sensing and idling. Recall that Θ_1 is the stationary probability that the PU is idle. Additionally, $\frac{q}{\Theta_1}\lambda$ represents the average delay cost. In (Stage-II), the SU uses the average channel gain $\overline{g}$ and the stationary channel idle probability Θ_1 to evaluate $H(V_k - t_{tr}r_k)$, which can be considered as the approximated aggregate cost to finish the remaining traffic volume $V_k - t_{tr}r_k$ in the future slots.

C. Backward Induction to solve the Two-stage Problem

We solve the above two-stage problem via the backward induction, i.e., we first solve problem (Stage-II) to evaluate $H(.)$, based on which we solve problem (Stage-I) for the rate-adaptation policy.

It can be verified that problem (Stage-II) is convex, and thus the first order optimality condition is applicable. Specifically, the optimality condition requires (we treat q as a continuous decision variable for nature of approximation)

$$2^{(\frac{V_k}{qt_{tr}} - \frac{r_k}{q})}\big(t_{tr}\frac{1}{\overline{g}} - \ln 2\frac{1}{\overline{g}}\frac{V_k - r_k t_{tr}}{q}\big) - t_{tr}\frac{1}{\overline{g}} + (\frac{1}{\Theta_1} - 1)\phi_{id}t_{tr} + \frac{1}{\Theta_1}\phi_{se}t_{se} + \lambda\frac{1}{\Theta_1} = 0. \quad (13)$$

Let $F(q) = 2^{(\frac{V_k}{qt_{tr}} - \frac{r_k}{q})}\big(t_{tr}\frac{1}{\overline{g}} - \ln 2\frac{1}{\overline{g}}\frac{V_k - r_k t_{tr}}{q}\big)$. It can be verified that $F(q)$ is increasing in q, and $F(q) - t_{tr}\frac{1}{\overline{g}} \leq 0$. Hence, a unique optimal solution exits for (13). We use $\hat{q}(r_k)$ (as a function the rate allocation) to denote the solution for problem (Stage-II). In spite of the complicated form of (13), we obtain the unique expression for $\hat{q}(r_k)$ as

$$\hat{q}(r_k) = (\frac{V_k}{t_{tr}} - r_k)C, \tag{14}$$

where C is a positive constant and satisfies the following condition

$$\Big(2^{\frac{1}{C}} - (\ln 2)2^{\frac{1}{C}}\frac{1}{C}\Big) = 1 - \frac{1}{\frac{1}{\overline{g}}t_{tr}}\big((\frac{1}{\Theta_1} - 1)\phi_{id}t_{tr} + \frac{1}{\Theta_1}\phi_{se}t_{se} + \lambda\frac{1}{\Theta_1}\big). \tag{15}$$

The detailed proof for (14) is given in the appendix. Let function $L(C) = 2^{\frac{1}{C}} - 1 - (\ln 2)2^{\frac{1}{C}}\frac{1}{C}$. It can be verified that $L(C)$ is increasing in C (as described in the appendix). Hence, a unique value of C exists.

Remark 4: (Evaluation of the Approximated Cost Function $H(.)$) Using $\hat{q}(r_k)$, after some manipulations of (13), the approximated aggregate cost to finish the remaining payload $V_k - t_{tr}r_k$ can be compactly given by

$$H(V_k - t_{tr}r_k) = \frac{1}{\overline{g}}(\ln 2)2^{\frac{V_k - r_k t_{tr}}{\hat{q}(r_k)t_{tr}}}(V_k - r_k t_{tr}). \tag{16}$$

□

Now we continue to solve problem (Stage-I). By putting (16) into the objective function of problem (Stage-I), we obtain

$$\min_{r_k} t_{se}\phi_{se} + t_{tr}\frac{1}{G_k}(2^{r_k} - 1) + \frac{1}{\overline{g}}\ln 2(V_k - r_k t_{tr})2^{\frac{1}{C}} + I_{[r_k=0]}\phi_{id}t_{tr} + \lambda I_{[V_k>0]}. \tag{17}$$

Since C is a constant, the above problem is convex. We denote the solution for problem (Stage-I) as $\hat{r}_k$, which can be given by

$$\hat{r}_k = \min\{\log_2(\frac{G_k}{\overline{g}}2^{\frac{1}{C}}), \frac{V_k}{t_{tr}}\}, \text{ when } S_k = 1. \tag{18}$$

Note that $\hat{r}_k = 0$, otherwise. In summary, we treat $\hat{r}_k$ given in (18) as the low-complexity policy from the CEC with approximation[8].

The low-complexity policy indicates a larger rate allocation when a better SU channel condition appears. This result is consistent with the optimal policy from the value iteration as shown in Fig. 2. Meanwhile, this result is also consistent with the principle of *opportunistic scheduling* (i.e., more aggressively using the channel opportunity under a better channel condition, and vice versa). Similar rationale (i.e., the rate allocation increases in $\frac{G_k}{\varrho}$, where ϱ denotes a scheduling threshold) also appeared in [21][9] [22]. However, neither of the suboptimal polices proposed in [21] [22] is applicable to CR due to the lack of consideration on the SU energy-overheads and the sensing error.

[8]Note that the only computational complexity in obtaining (18) stems from solving (15) for C numerically. With the bisection method, C can be found within $\ln\frac{\overline{C}-\underline{C}}{\epsilon}$ iterations, where $\overline{C}$ and $\underline{C}$ represent the upper and lower bounds of the value of C, respectively. ϵ is the tolerable error.

[9]Note that the suboptimal policy proposed in [21] considered a hard delay constraint, which may not be feasible for the SU because the CR does not have its own licensed channel always available to use. Consequently, it is crucial to determine how long (on average) the SU needs to finish its payload as shown by our problem (Stage-II).

D. Evaluation of the Impact of the System Parameters

We remark the low-complexity policy regarding the impact of the PU activity, the SU energy-overheads, and the SU delay sensitivity as follows.

Remark 5: (Impact of the PU Activity) Condition (15) requires that the value of C increases in the PU idle probability Θ_1. Thus, $\hat{r}_k$ decreases in Θ_1, i.e., the SU transmits slower if more idle spectrum opportunities exist. As $\Theta_1 \to 1$ (i.e., the PU is always idle), then the sensing power is the only overhead faced by the SU, and the SU can slow down its transmission without any energy consumption in compulsory idling (note that the SU still consumes energy for the spectrum sensing). □

Remark 6: (Impact of the SU Sensing Overheads) The parameter C in (18) characterizes the impact of energy-overheads on the SU rate allocation. Since function $L(C)$ is increasing in C, condition (15) indicates that the value of C decreases in the sensing power ϕ_{se} and the idling power ϕ_{id}. Therefore, $\hat{r}_k$ increases accordingly. This result is consistent with the previous result from the optimal policy showing that the SU tends to transmit faster to save its energy consumption under a larger sensing power (idling power). Furthermore, we can quantify that

$$\frac{\partial\hat{r}_k}{\partial\phi_{se}} = \frac{t_{se}}{\Theta_1}\frac{1}{\frac{1}{\overline{g}}t_{tr}(\ln 2)^2}\frac{1}{\frac{1}{C}2^{\frac{1}{C}}} > 0, \tag{19}$$

which indicates that the marginal impact of the sensing power ϕ_{se} decreases in ϕ_{se}, because C decreases in ϕ_{se}. Similar results also hold for the idling power ϕ_{id}, and the marginal impact of ϕ_{id} is quantified by $\frac{\partial\hat{r}_k}{\partial\phi_{id}} = (\frac{1}{\Theta_1} - 1)\frac{1}{\frac{1}{\overline{g}}(\ln 2)^2}\frac{1}{\frac{1}{C}2^{\frac{1}{C}}} > 0$, which also diminishes in ϕ_{id}. □

Figure 4 shows performance of the optimal policy and the low-complexity policy with $\lambda = 0$ (in the two top-subfigures) and with $\lambda = 2$ (in the two bottom-subfigures), respectively. Specifically, we consider a slowly-varying Rayleigh fading channel with unit average gain and the fading rate equal to 0.025 (the fading rate depends on both the maximum Doppler frequency and the block period [22] [26]). We model this Rayleigh fading channel as a 8-state FSMC with the similar equal-probability partitioning approach as [22] [26].

For a more detailed comparison, we also consider a *baseline* policy in which the SU transmits with a constant transmit rate when the PU is idle. In particular, we consider two cases of the baseline policy with constant rates equal to 2 and 5, respectively. The left subfigure shows that both the optimal policy and low-complexity policy perform much better than the baseline policies in terms of average total cost. As described before, the optimal policy achieves the best tradeoff between the energy consumption for effective data transmission and the corresponding energy-overheads, and thus yields the minimum average total cost. Furthermore, the right subfigure shows that the low-complexity policy achieves

comparable performance as the optimal policy. In all of our numerical results, the low-complexity policy shows comparable performance as that of the optimal policy, especially when the target traffic volume $V^{\max}$ is large (e.g., $V^{\max} \geq 40$)[10]. Since the baseline policy shows apparently inferior performance compared to both the optimal policy and the low-complexity policy, we shall focus on performance comparison between the optimal policy and the low-complexity policy for clear presentation in the following.

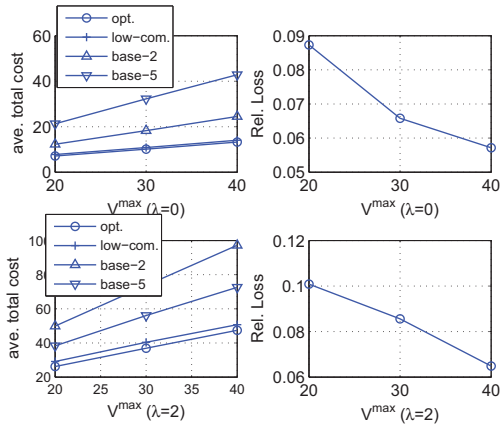

Fig. 4. Performance comparison of the optimal policy, the low-complexity policy and the baseline policy. We set $\phi_{se} = 2, t_{se} = 0.2$. $\phi_{id} = 0.1$, $t_{tr} = 1$. We consider two different baseline policies with the constant transmit rates equal to 2 and 5 (when the PU is idle), respectively. The two subfigures on the top are with $\lambda = 0$. The two sbufigures at the bottom are with $\lambda = 2$. The two subfigures on the left column show the average total cost of the optimal policy, the low-complexity policy and the baseline policy. The two subfigures on the right column show the relative loss of the low-complexity policy compared to the optimal policy. For fair comparison with the optimal policy, we set the low-complexity policy as $\left[\log_2(\frac{G_k}{\bar{g}} 2^{\frac{1}{C}})\right]_{\mathbb{R}(S_k)}$ in the numerical illustrations, where $[x]_{\mathbb{R}(.)}$ represents the feasible rate allocation in set $\mathbb{R}(.)$ that is the closest to x.

Remark 7: (Impact of Delay Sensitivity of the SU Traffic) The parameter C also characterizes the impact of the delay cost λ on the SU rate allocation. Specifically, condition (15) requires that C decreases in λ. Therefore, $\hat{r}_k$ increases with a large delay cost λ. This is consistent with the intuition that the SU transmits faster for delay-sensitive traffic. Moreover, the marginal impact of λ can be quantified as $\frac{\partial \hat{r}_k}{\partial \lambda} = \frac{1}{\frac{1}{C} 2^{\frac{1}{C}}} \frac{1}{t_{tr} \frac{1}{\bar{g}} (\ln 2)^2} \frac{1}{\Theta_1} > 0$, i.e., its marginal impact diminishes with the increase of λ. The left subfigure in Fig. 5 verifies this point. Specifically, the smaller the λ, the larger the increase in the average delay. By tuning λ, we obtain the Pareto optimal boundary for the average traffic delay versus the average energy consumption.

Remark 8: (Impact of Energy Overheads under Different Levels of Traffic Sensitivity) Since C decreases in the delay cost λ, the marginal impact of the SU energy-overhead will be significant if the SU delay cost λ is small according to (19). The left subfigure in Fig. 5 verifies this point. Specifically, when λ is small (i.e., for delay-insensitive traffic), a large difference appears between the result with small energy-overheads (i.e., $\phi_{se} = 2$,$\phi_{id} = 0.1$) and the result with large energy-overheads (i.e., $\phi_{se} = 4$,$\phi_{id} = 0.3$). In comparison, a small difference appears when λ is large (i.e., for delay-sensitive traffic). Meanwhile, clear tradeoffs between the SU average energy consumption and the average traffic delay exhibit (via tuning the delay cost λ) under different SU energy-overheads. The right subfigure in Fig. 5 further shows the relative loss in terms of the average total cost of the low-complexity policy compared to that of the optimal policy. Small relative losses (no greater than 10%) appear under all the tested delay costs and energy-overheads.

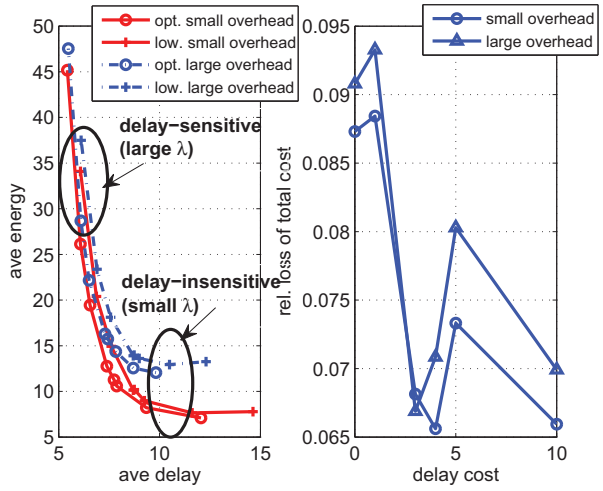

Fig. 5. Performance comparison between the low-complexity policy and the optimal policy under different delay sensitivities and different energy-overheads. Left subfigure: the Pareto optimal boundary for the average traffic delay versus the average energy consumption. We consider two cases of energy-overheads, i.e., small energy-overheads with $(\phi_{se} = 2, \phi_{id} = 0.1)$ and large energy overheads with $(\phi_{se} = 4, \phi_{id} = 0.3)$. Right subfigure: relative loss in terms of the average total cost of the low-complexity policy compared to that of the optimal policy.

E. Performance Evaluation

We analyze the performance of the low-complexity policy. The following lemma first provides an approximation of the average delay performance when using the low-complexity policy. The proof is given in the appendix.

Lemma *2: (Average Delay with the Low-Complexity Policy)* Using the low-complexity rate-adaptation policy in (18), the average number of slots for the SU to finish the payload $V^{\max}$ is lower bounded by

$$\overline{D}_{\text{low}} = \frac{V^{\max}}{t_{tr} \sum_{g \in \mathcal{G}} \eta_g \log_2(\frac{g}{\bar{g}} 2^{\frac{1}{C}})} \frac{1}{\Theta_1}. \tag{20}$$

Furthermore, the bound is asymptotically tight as $V^{\max} \to \infty$. □

The top subfigure in Fig. 6 verifies this point by showing the relative difference between (20) and the numerical results

[10]The results in both Fig. 2 and Fig. 7 indicate that, according to the optimal policy, the remaining payload v has little impact on the SU rate allocation as v is relatively large. Therefore, our low-complexity policy (18) still can achieve comparable performance as the optimal policy, even though the information on v is not fully utilized (especially when its target payload $V^{\max}$ is large). Notice that similar phenomenon was also observed by [13] showing that the SU remaining energy level had little influence on its sensing and access decisions under a large remaining energy level.

of the low-complexity policy. Based on (20), the following lemma further approximates the average energy consumption when using the low-complexity policy. The proof is given in the appendix.

Lemma *3: (Average Energy Consumption with the Low-Complexity Policy)* Using the low-complexity rate-adaptation policy in (18), the average energy consumption for the SU to finish its target payload $V^{\max}$ can be approximated by

$$\overline{E} = \frac{V^{\max}}{t_{tr}\sum_{g\in\mathcal{G}}\eta_g \log_2(\frac{g}{\bar{g}}2^{\frac{1}{C}})}\frac{\Theta_0}{\Theta_1}(t_{se}\phi_{se}+t_{tr}\phi_{id}) + \frac{V^{\max}}{t_{tr}\sum_{g\in\mathcal{G}}\eta_g \log_2(\frac{g}{\bar{g}}2^{\frac{1}{C}})}\Big(\sum_{g\in\mathcal{G}}\eta_g(t_{tr}\phi_{tx}(\hat{r},g)+t_{se}\phi_{se})\Big). \quad (21)$$

Furthermore, the approximation is asymptotically accurate as $V^{\max}\to\infty$. □

Note that $\hat{r}$ in (21) is a function of the channel gain state g according to the low-complexity policy (18). Without causing any ambiguity, we omit g for clarity. The bottom subfigure in Fig. 6 shows the relative difference between (21) and the numerical results of the low-complexity policy. The results in both subfigures indicate the asymptotic accuracy of (20) and (21).

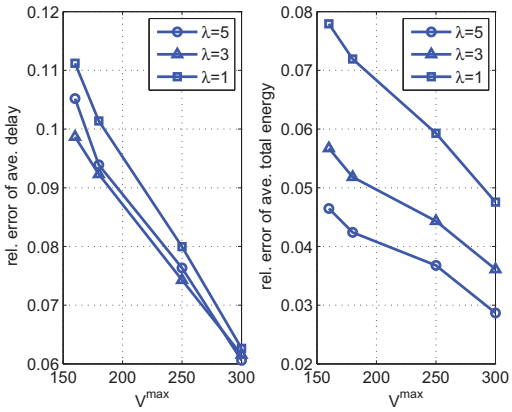

Fig. 6. Performance analysis of the low-complexity policy using (20) and (21). We consider three different traffic sensitivities, i.e., $\lambda = 1, 3, 5$. Left subfigure: relative error of the traffic delay lower bound (20) compared to the numerical result from the low-complexity policy. Right subfigure: relative error of the approximated energy consumption (21) compared to the numerical result from the low-complexity policy.

V. SU Rate-Adaptation under the Imperfect Spectrum Sensing

In this section we consider the impact of imperfect spectrum sensing. We first incorporate the spectrum sensing error into our previous MDP formulation in section III and derive the corresponding optimal policy for the SU rate adaptation. We then incorporate the imperfect spectrum sensing into our low-complexity policy. We shall quantify the impact of imperfect spectrum sensing on the SU rate adaptation.

A. Optimal Policy under Imperfect Spectrum Sensing

In practice, the spectrum sensing is imperfect, which can be represented by the mis-detection probability $p_{md} = \Pr\{\widetilde{S}_k = 1|S_k = 0\} > 0$ and the false alarm probability $p_{fa} = \Pr\{\widetilde{S}_k = 0|S_k = 1\} > 0$[11]. We use $\widetilde{S}_k$ to denote the SU sensing result, which may differ from the PU true state S_k due to the sensing error. Note that in the previous sections, we use "the SU sensing result" and "the PU state" interchangeably since the perfect spectrum sensing is assumed. However, in section V, we explicitly differentiate them using $\widetilde{S}_k$ and S_k, respectively, due to the existence of sensing error. Specifically, the one-step transition probability of the SU sensing result process $\{\widetilde{S}_k\}$ can be given by (22) on the top of the next page. Note that $\Pr\{\widetilde{S}_{k+1} = y'|S_{k+1} = y\}$ and $\Pr\{\widetilde{S}_k = x'|S_k = x\}$ only depend on the SU sensing accuracy. We assume that the SU sensing accuracy is time homogeneous, i.e., the sensing accuracy is not time-correlated. Thus, Markov property still holds for the process of SU sensing result $\{\widetilde{S}_k\}$, which we can treat as a Markov chain. The corresponding one-step transition probability is determined by both the PU activity and the SU sensing accuracy according to (22)[12]. For clarity, let $\vartheta_{\widetilde{s}\widetilde{s}'} = \Pr\{\widetilde{S}_{k+1} = \widetilde{s}'|\widetilde{S}_k = \widetilde{s}\}, \forall \widetilde{s}, \widetilde{s}' \in \mathcal{S} = \{0, 1\}$. In this section, we assume that assumption 3 in section II-B holds even under the SU spectrum sensing error. The assumption is reasonable because according to [33], the SU is required to detect the PU activity under typically low SNR region (for strict incumbent protection), which is more stringent than that for the SU channel estimation (especially when the SU adopts some advanced pilot-based channel estimation techniques [25]). More importantly, this assumption helps to separate the impact of imperfect spectrum sensing from that of the imperfect channel estimation, and thus facilitating our following analysis[13].

Our previous formulation with the stochastic shortest path MDP in section III can be extended to include the imperfect spectrum sensing. Specifically, the system state is now denoted by $(\widetilde{S}_k, G_k, V_k)$. The action space $\mathbb{R}(.)$ and the per-slot cost (1) in section III still remain unchanged. However, the transition kernel under the imperfect spectrum sensing is now given by

$$\Pr\{(\widetilde{s}', g', v')|(\widetilde{s}, g, v)\} = \begin{cases} \vartheta_{\widetilde{s}\widetilde{s}'}\eta_{gg'}\Pr\{r|(s,g,v)\}I_{[v'=v-rt_{tr}]}\Pr\{s=1|\widetilde{s}=1\}, \\ \qquad\qquad \text{if } v>0, r\neq 0 \\ \vartheta_{\widetilde{s}\widetilde{s}'}\eta_{gg'}\Pr\{r|(s,g,v)\}I_{[v'=v]}\Pr\{s=0|\widetilde{s}=1\}, \text{ if } v>0, r=0 \\ \vartheta_{\widetilde{s}\widetilde{s}'}\eta_{gg'}I_{[v'=v]}, \text{ otherwise} \end{cases}.$$

Specifically, the second case in (23) represents that a mis-detection happens, and thus the transmission of the SU collides with that of the PU. We assume that the SU transmitted data is lost when colliding with the PU, and thus the SU has to do retransmission in the future slots. For example, the SUTx infers that a collision has happened if it does not receive any ACK from the SURx at the end of the slot. Therefore, the

[11] For convenience in manipulation, we frequently use the detection probability $p_{de} = 1 - p_{md}$ in the rest of this work.

[12] Similar Markov chain modeling the SU sensing result process also appeared in [20]. Another model that incorporates the SU sensing error is based on the Partially Observable Markov Decision Process, which is out of the scope of this paper.

[13] Similar assumption also appeared in [30] to analyze the SU selective channel access.

$$\Pr\{\widetilde{S}_{k+1}=y'|\widetilde{S}_k=x'\}=\frac{\sum_x\sum_y \Pr\{\widetilde{S}_{k+1}=y'|S_{k+1}=y\}\Pr\{\widetilde{S}_k=x'|S_k=x\}\Pr\{S_k=x\}\Pr\{S_{k+1}=y|S_k=x\}}{\Pr\{\widetilde{S}_k=x'|S_k=x\}\Pr\{S_k=x\}}. \quad (22)$$

modified MDP problem with the imperfect spectrum sensing is given by

$$\textbf{(P4):}\ \min_{\pi}\mathbb{E}\{\sum_{k=1}^{\hat{K}} c(\widetilde{S}_k,G_k,V_k,r_k)|(\widetilde{S}_1,G_1,V^{\max})\}. \quad (23)$$

Remark 9: (Impact of Sensing Error on the Optimal Policy) The impact of the SU sensing error are two-fold, (i) the false alarm (i.e., $p_{fa}>0$) causes the waste of idle spectrum opportunities, which results in the SU spending more energy-overheads in sensing and idling, and (ii) the mis-detection (i.e., $p_{md}>0$) causes the energy waste in data transmission (due to collision), which results in the SU spending extra energy for re-transmission. Figure 7 shows the optimal rate allocation profile for this modified MDP problem with the sensing error. The two top-subfigures are with the detection probabilities $p_{de}=1$ and $p_{de}=0.8$, respectively. The two bottom-subfigures are with the false alarm probabilities $p_{fa}=0$ and $p_{fa}=0.2$, respectively. The results indicate that the SU optimal rate decreases (increases) with the increase of its mis-detection (false-alarm) probability.□

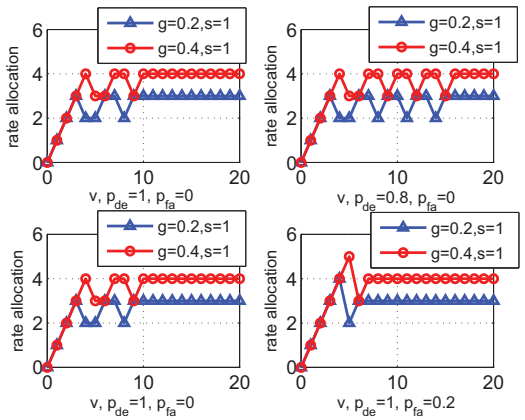

Fig. 7. The optimal rate allocation profile under imperfect spectrum sensing. We set $\phi_{se}=1,\phi_{id}=0.1$, and $\lambda=0$. The same representative two-state channel model as in Fig. 2 is used. Top two subfigures: the optimal rate allocation profiles under two different detection probabilities $p_{de}=1$ (top-left) and $p_{de}=0.8$ (top-right). Bottom two subfigures: the optimal rate allocation profile under two different false alarm probabilities $p_{fa}=0$ (bottom-left) and $p_{fa}=0.2$ (bottom-right).

B. Low-Complexity Policy under the Imperfect Spectrum Sensing

We incorporate the imperfect spectrum sensing into our low-complexity policy. The low-complexity rate-adaptation problem is still formulated as a two-stage problem. Specifically, in (Stage-II), the expected total cost to finish the remaining payload $V_k-t_{tr}r_k$ under the spectrum sensing error can be given by

$$H(V_k-t_{tr}r_k)=$$
$$\min_q\big(q+\frac{q}{1-p_{fa}}\frac{\Theta_0}{\Theta_1}(1-p_{de})\big)t_{tr}(2^{\frac{V_k-r_kt_{tr}}{qt_{tr}}}-1)\frac{1}{\bar{g}}+$$
$$\frac{q}{\Theta_1(1-p_{fa})}t_{se}\phi_{se}+\big(\frac{q}{1-p_{fa}}p_{fa}+\frac{q}{1-p_{fa}}\frac{\Theta_0}{\Theta_1}p_{de}\big)\phi_{id}t_{tr}+$$
$$\lambda\frac{q}{\Theta_1(1-p_{fa})}. \quad (24)$$

The first item includes both the SU energy consumption in data transmission and the corresponding energy waste due to mis-detection. The third item includes both the SU energy consumption in idling and the corresponding waste due to false alarm. The solution to (24) can be compactly given by $\hat{q}(r_k)=(\frac{V_k}{t_{tr}}-r_k)C$, where the positive parameter C satisfies the following condition

$$\big((2^{\frac{1}{C}}-1)-2^{\frac{1}{C}}\ln 2\frac{1}{C}\big)+M(p_{de},p_{fa})=0, \quad (25)$$

and function $M(p_{de},p_{fa})$ is given by

$$M(p_{de},p_{fa})=\frac{1}{\big(1+\frac{1}{1-p_{fa}}\frac{\Theta_0}{\Theta_1}(1-p_{de})\big)t_{tr}\frac{1}{\bar{g}}}\times$$
$$\{\frac{1}{\Theta_1(1-p_{fa})}\phi_{se}t_{se}+(\frac{p_{fa}}{1-p_{fa}}+\frac{1}{1-p_{fa}}\frac{\Theta_0}{\Theta_1}p_{de})\phi_{id}t_{tr}+$$
$$\lambda\frac{1}{\Theta_1(1-p_{fa})}\}. \quad (26)$$

The detailed proof is similar to that for (14), and we do not repeat it here. Specifically, it can be verified that $M(p_{de},p_{fa})$ is increasing in both p_{de} and p_{fa}[14].

Remark 10: (Evaluation of the Approximated Cost $H(.)$ under the Imperfect Spectrum Sensing) By using $\hat{q}(r_k)$, the approximated aggregate cost to finish the remaining payload $V-t_{tr}r_k$ under the spectrum sensing error can be given by

$$H(V_k-t_{tr}r_k)=$$
$$\big(1+\frac{1}{1-p_{fa}}\frac{\Theta_0}{\Theta_1}(1-p_{de})\big)\frac{1}{\bar{g}}(\ln 2)2^{\frac{V_k-r_kt_{tr}}{\hat{q}(r_k)t_{tr}}}(V_k-r_kt_{tr}). \quad (27)$$

Next, we continue to solve problem (Stage-I). Specifically, given the system state $(\widetilde{S}_k,G_k,V_k)$, the rate allocation problem in (Stage-I) is formulated as

$$\min_{r_k}t_{se}\phi_{se}+t_{tr}\frac{1}{G_k}(2^{r_k}-1)+H(V_k-t_{tr}r_k)\Pr\{S=1|\widetilde{S}=1\}$$
$$+H(V_k)\Pr\{S=0|\widetilde{S}=1\}+I_{[r_k=0]}\phi_{id}t_{tr}+\lambda I_{[V_k>0]},\text{if }\widetilde{S}_k=1. \quad (28)$$

Different from (11), the fourth item in (28) represents the expected cost when the SU mis-detects the presence of the

[14]Let $\widetilde{\Theta}_1=\Pr\{\widetilde{S}_k=1\}$ ($\widetilde{\Theta}_0=\Pr\{\widetilde{S}_k=0\}$) denote the stationary probability that the SU sensing result is idle (busy). Based on the knowledge on its own sensing accuracy (i.e., the values of p_{de} and p_{fa}), the SU can infer the PU true idle (busy) probability Θ_1 (Θ_0).

PU. The solution to problem (28) can be compactly given by

$$\hat{r}_k = \min\{\log_2(\frac{G_k}{\overline{g}} 2^{\frac{1}{C}}), \frac{V^{\max}}{t_{tr}}\} \text{ when } \widetilde{S}_k = 1, \qquad (29)$$

and $\hat{r}_k = 0$, otherwise. We call $\hat{r}_k$ (29) the SU low-complexity policy under the sensing error. The low-complexity policy (29) shares the same form as (18) under the perfect spectrum sensing. However, the key difference between them lies in the parameter C (given by (25)), which now characterizes the impact of p_{de} and p_{fa}.

Remark 11: (Impact of Sensing Error on the SU Rate Adaptation) Since $M(p_{de}, p_{fa})$ is increasing in p_{de} (p_{fa}), thus condition (25) indicates that the value of C decreases in p_{de} (p_{fa}). Further according to (29), we can quantify the marginal impacts of p_{de} as $\frac{\partial \hat{r}_k}{\partial p_{de}} = \frac{1}{\frac{1}{C} 2 \frac{1}{C}} \frac{1}{t_{tr} \frac{1}{g} (\ln 2)^2} \frac{\Theta_0}{(\widetilde{\Theta}_1)^2} (\phi_{id} t_{tr} + \phi_{se} t_{se} + \lambda) > 0$, and the marginal impact of p_{fa} as $\frac{\partial \hat{r}_k}{\partial p_{fa}} = \frac{1}{\frac{1}{C} 2 \frac{1}{C}} \frac{1}{t_{tr} \frac{1}{g} (\ln 2)^2} \frac{\Theta_1}{(\widetilde{\Theta}_1)^2} (\phi_{id} t_{tr} + \phi_{se} t_{se} + \lambda) > 0$, meaning that the SU rate allocation $\hat{r}_k$ decreases (increases) in p_{md} (p_{fa}). These results can be explained by the following two points. First, with a larger mis-detection probability p_{md}, the SU faces a larger risk in wasting its energy in data transmission. Thus, the SU decreases its rate accordingly. Second, with a larger false alarm probability p_{fa}, the SU suffers a larger energy-overhead (due to both spectrum sensing and unnecessary idling). Thus, the SU tends to increase its rate to finish its payload sooner. These results are consistent with the optimal policy for the modified MDP formulation as shown in Fig. 7. Figure 8 further shows the relative loss (in terms of the average total cost) of the low-complexity policy under the sensing error compared to the optimal policy under the sensing error, thus validating that our low-complexity policy achieves comparable performance as the optimal policy. □

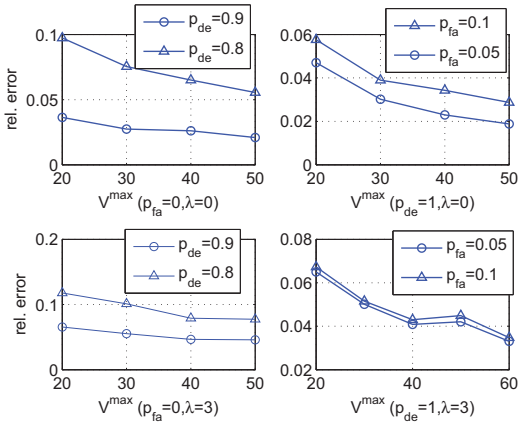

Fig. 8. Performance comparison between the optimal policy and the low-complexity policy under the imperfect sensing. The top two subfigures are with the delay cost $\lambda = 0$. The top-left subfigure shows the performance under different p_{de}. The top-right subfigure shows the performance under different p_{fa}. The bottom two subfigures are with $\lambda = 3$. The bottom-left subfigure shows the performance under different p_{de}. The bottom-right subfigure shows the performance under different p_{fa}. All the numerical results show that our low-complexity policy under the imperfect spectrum sensing still achieves comparable performance as the optimal policy, especially when $V^{\max}$ is large.

C. Performance Evaluation under the Imperfect Spectrum Sensing

The marginal impact of the SU energy-overheads under the imperfect spectrum sensing can also be quantified according to (29). Specifically, the marginal impact of ϕ_{se} is $\frac{\partial \hat{r}_k}{\partial \phi_{se}} = \frac{1}{\frac{1}{C} 2 \frac{1}{C}} \frac{1}{t_{tr} \frac{1}{g} (\ln 2)^2} \frac{t_{se}}{\Theta_1(1-p_{fa}) + \Theta_0(1-p_{de})} > 0$. The marginal impact of ϕ_{id} is $\frac{\partial \hat{r}_k}{\partial \phi_{id}} = \frac{1}{\frac{1}{C} 2 \frac{1}{C}} \frac{1}{\frac{1}{g} (\ln 2)^2} \frac{\Theta_1 p_{fa} + \Theta_0 p_{de}}{\Theta_1(1-p_{fa}) + \Theta_0(1-p_{de})} > 0$. Meanwhile, the marginal impact of the SU delay cost is $\frac{\partial \hat{r}_k}{\partial \lambda} = \frac{1}{\frac{1}{C} 2 \frac{1}{C}} \frac{1}{t_{tr} \frac{1}{g} (\ln 2)^2} \frac{1}{\Theta_1(1-p_{fa}) + \Theta_0(1-p_{de})} > 0$. All these results are consistent with the previous results in section IV when $p_{de} = 1$ and $p_{fa} = 0$.

Based on the low-complexity policy under the sensing error, we evaluate the SU average traffic delay of in the following lemma. The proof is similar to that of Lemma 2, and it further takes account of the SU spectrum sensing error.

Lemma *4: (Average Delay with the Low-Complexity Policy under the Sensing Error)* Using the low-complexity rate-adaptation policy (29) under the sensing error, the average number of slots for the SU to finish its target payload $V^{\max}$ is lower bounded by

$$\overline{D}_{\text{low}} = \frac{V^{\max}}{t_{tr} \sum_{g \in \mathcal{G}} \eta_g \log_2(\frac{g}{\overline{g}} 2^{\frac{1}{C}})} \frac{1}{\Theta_1(1-p_{fa})}. \qquad (30)$$

Furthermore, the bound is asymptotically tight as $V^{\max} \to \infty$. In particular, comparison between (30) and (20) indicates the additional delay the SU suffers due to the sensing error. This additional delay diminishes as $p_{de} \to 1$ and $p_{fa} \to 0$. □

Further based on the average delay (30), we evaluate the average energy consumption of the SU in the following Lemma 5. The proof is similar to that of Lemma 3, and it further takes account of the mis-detection (which causes the waste of energy in data transmission) and the false alarm (which causes the waste of energy in unnecessary idling).

Lemma *5: (Average Energy Consumption with the Low-Complexity Policy under the Sensing Error)* Using the low-complexity rate-adaptation policy in (29) under the sensing error, the average energy for the SU to finish its target payload $V^{\max}$ can be approximated by

$$\overline{E} = \frac{V^{\max}}{t_{tr} \sum_{g \in \mathcal{G}} \eta_g \log_2(\frac{g}{\overline{g}} 2^{\frac{1}{C}})} \big(\frac{p_{fa}}{1-p_{fa}} + \frac{\Theta_0 p_{de}}{\Theta_1(1-p_{fa})}\big) \times (t_{se}\phi_{se} + t_{tr}\phi_{id}) + \frac{V^{\max}}{t_{tr} \sum_{g \in \mathcal{G}} \eta_g \log_2(\frac{g}{\overline{g}} 2^{\frac{1}{C}})} \big(1 + \frac{\Theta_0(1-p_{de})}{\Theta_1(1-p_{fa})}\big) \times \big(\sum_{g \in \mathcal{G}} \eta_g (t_{tr}\phi_{tx}(\hat{r}, g) + t_{se}\phi_{se})\big). \qquad (31)$$

Furthermore, the approximation is asymptotically accurate as $V^{\max} \to \infty$. In particular, comparison between (31) and (21) indicates the additional energy consumption that the SU suffers when $\widetilde{\Theta}_0 \geq \Theta_0$[15] due to the sensing error. This additional consumption diminishes as $p_{de} \to 1$ and $p_{fa} \to 0$. □

Figure 9 shows comparison between our performance evaluations using (30) and (31) and the corresponding numerical

[15]This condition indicates that the stationary probability of the SU sensing result being busy will be larger than the stationary probability of the PU true state being busy, i.e., the SU suffers a waste of idle spectrum opportunity due to sensing error.

results under different detection probabilities. Figure 10 further shows the corresponding comparison under different false-alarm probabilities. All these results validate that the performance evaluations using (30) and (31) are asymptotically accurate as $V^{\max}$ increases.

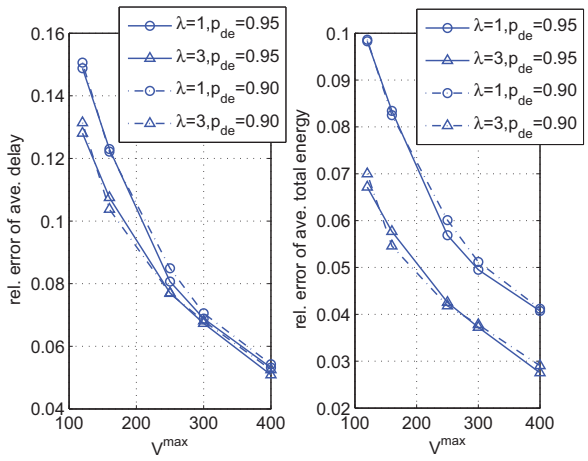

Fig. 9. Performance evaluation of our low-complexity policy using (30) and (31) under different detection probabilities. We set $\phi_{se} = 1$, $\phi_{id} = 0.1$ and the false alarm probability $p_{fa} = 0$. Left-subfigure: relative error between the approximated delay (30) and the numerical results under different delay costs. Right-subfigure: relative error between the approximated energy consumption (31) and the numerical results under different delay costs. All of the results indicate that our performance evaluations (30) and (31) are asymptotically accurate as $V^{\max}$ increases.

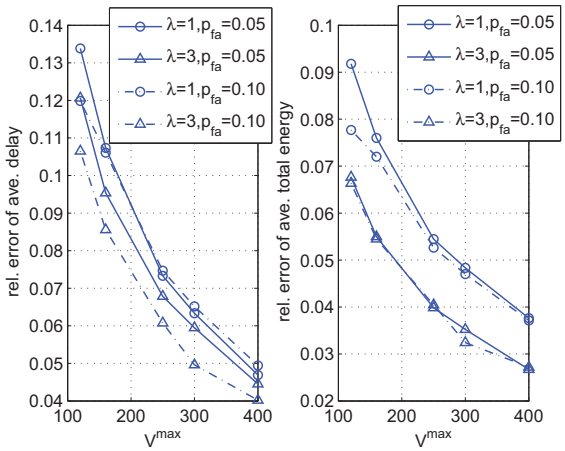

Fig. 10. Performance evaluation of our low-complexity policy using (30) and (31) under different false alarm probabilities. We set $\phi_{se} = 1$, $\phi_{id} = 0.1$ and the detection probability $p_{de} = 1$. Left-subfigure: relative error between the approximated delay (30) and the numerical results under different delay costs. Right-subfigure: relative error between the approximated energy consumption (31) and the numerical results under different delay costs. All of the results indicate that our performance evaluations (30) and (31) are asymptotically accurate as $V^{\max}$ increases.

VI. Conclusion

Energy-efficient transmission of CR requires an appropriate balance between the energy consumption for effective data transmission and that for spectrum sensing and compulsory idling. We thus formulate the problem of energy-efficient transmission and sensing as a stochastic shortest path MDP in which the SU aims at minimizing its average cost (including both energy consumption and the delay cost) to finish a target payload. To avoid high computational complexity in deriving the optimal policy, we propose a low-complexity rate-adaptation policy which achieves comparable performance as the optimal policy. Based on the low-complexity policy, we further quantify the impact of sensing and idling power consumption on the SU rate allocation, and show the corresponding tradeoff between the average SU energy consumption and the average traffic delay under different energy-overheads. Our results show that to minimize its average cost, the SU rate increases in its energy-overheads, whose marginal impact, however, diminishes. Meanwhile, the marginal impact of energy-overheads is more significant for delay-insensitive traffic than that for delay-sensitive traffic. We further consider the impact of imperfect spectrum sensing, and our results quantify that the SU decreases (increases) its rate with the increase of mis-detection probability (false alarm probability).

Appendix: Proof of Theorem 1

Proof of Theorem 1: First, for a unconstrained MDP problem, a *deterministic* policy (i.e., the optimal action is a *deterministic* function of the system state) suffices to be optimal [34]. Second, in problem (P2), the SU will eventually finish its payload (i.e., reaching the terminal state) within a finite time for the following two reasons: (i) the sensing spectrum introduces energy consumption at each slot, and (ii) the idling introduces energy consumption when $S_k = 0$. Suppose that the SU will not complete the delivery of its payload within a finite time, then the SU energy consumption will be infinite, which is obviously inferior to finishing $V^{\max}$ within a finite duration. In other words, problem (P2) is equivalent to a stochastic shortest path problem. Moreover, the following two properties hold for our problem (P2), namely, (i) the per-slot cost (1) is strictly positive except that at the terminal state, and (ii) the optimal cost $J(s, g, v), \forall (s, g, v)$ is finite (note that because of these two properties, the proof of the optimal stationary policy for (P2) allows the existence of *improper* admissible strategies [36]). Therefore, Proposition 7.2.1 [36] is applicable to our problem, and the existence of optimal stationary policy follows. □

Appendix: Proof of Lemma 1

Proof of Lemma 1: Let π^* denote the optimal policy for problem (P2) with the delay cost λ, i.e., policy π^* satisfies condition (5) from the *Bellman's equations*. Consider another

policy π' that does not satisfy condition (5). There exists

$$\mathbb{E}\{\sum_{k=1}^{\infty} c_E(S_k,G_k,V_k,r_k)|(S_1,G_1,V^{\max}),\pi^*\} +\mathbb{E}\{\sum_{k=1}^{\infty}\lambda I_{[V_k>0]},\pi^*\} \leq \mathbb{E}\{\sum_{k=1}^{\infty} c_E(S_k,G_k,V_k,r_k)|(S_1,G_1,V^{\max}),\pi'\} +\mathbb{E}\{\sum_{k=1}^{\infty}\lambda I_{[V_k>0]},\pi'\}, \quad (32)$$

where the left hand side of (32) is based on the optimal policy π^*, and the right hand side of (32) is based on policy π'. Suppose that the delay constraint (6) is binding when policy π^* is adopted, i.e., $\mathbb{E}\{\sum_{k=1}^{\infty} I_{[V_k>0]},\pi^*\} = \overline{D}$. Then, the above result (32) indicates that

$$\mathbb{E}\{\sum_{k=1}^{\infty} c_E(S_k,G_k,V_k,r_k)|(S_1,G_1,V^{\max}),\pi^*\} \leq \mathbb{E}\{\sum_{k=1}^{\infty} c_E(S_k,G_k,V_k,r_k)|(S_1,G_1,V^{\max}),\pi'\} + \lambda\big(\mathbb{E}\{\sum_{k=1}^{\infty} I_{[V_k>0]},\pi'\} - \overline{D}\big). \quad (33)$$

Since $\mathbb{E}\{\sum_{k=1}^{\infty} I_{[V_k>0]},\pi'\} \leq \overline{D}$ holds for any feasible policy π' for problem (P3), the above result (33) indicates that policy π^* is also optimal for problem (P3) with the delay cost λ interpreted as the corresponding Lagrangian multiplier. □

APPENDIX: PROOF OF THEOREM 2

Proof of Theorem 2: The cost $J(s,g,v)$ denotes the minimum cost to finish the payload v starting from the system state (s,g). Therefore, with a larger sensing power ϕ_{se} (or idling power ϕ_{id}), a larger optimal cost $J(s,g,v)$ is required.

To prove that $r^*(1,g,v,\phi_{se})$ is nondecreasing in ϕ_{se}, we virtually treat ϕ_{se} as one of the components of the system state, i.e., the system state now is augmented as (s,g,v,ϕ_{se}). Specifically, we set ϕ_{se} as a random variable which follows an independent and identical distribution at each slot. Arbitrary distribution for ϕ_{se} at each slot is applicable here. Let $\Omega_{\phi_{se}}$ denote the set of values for ϕ_{se}. By restricting $\Omega_{\phi_{se}}$ as a singleton set, we obtain the *original* result when ϕ_{se} is fixed. In comparison, by extending $\Omega_{\phi_{se}}$ to have several nonequal members, we can evaluate the impact of ϕ_{se} on the optimal decision. The property that $r^*(1,g,v)$ is nondecreasing in ϕ_{se} is established by showing that the augmented Q-factor $Q(s,g,v,\phi_{se},r)$ is submodular in (ϕ_{se},r) [23] [35]. The same method is also applicable to ϕ_{id}. The detailed proof is as follows.

Let a and b denote two feasible rate allocations with $a \geq b$. We aim to show that $Q(s,g,v,\phi_{se},a) - Q(s,g,v,\phi_{se},b)$ is decreasing in ϕ_{se}[16]. Specifically, there exists

$$Q(s,g,v,\phi_{se},a) - Q(s,g,v,\phi_{se},b) = c(s,g,v,\phi_{se},a) + \sum_{s'}\sum_{g'}\sum_{\phi'_{se}}\theta_{ss'}\eta_{gg'}\Pr(\phi'_{se})J(s',g',v-at_{tr},\phi'_{se}) -c(s,g,v,\phi_{se},b) - \sum_{s'}\sum_{g'}\sum_{\phi'_{se}}\theta_{ss'}\eta_{gg'}\Pr(\phi'_{se})J(s',g',v-bt_{tr},\phi'_{se}). \quad (34$$

In order to show that (34) is decreasing in ϕ_{se}, it is sufficient to show that (i) the per-slot cost $c(s,g,v,\phi_{se},r)$ is submodular in (ϕ_{se},r), and (ii) $J(s',g',v-bt_{tr},\phi'_{se}) - J(s',g',v-at_{tr},\phi'_{se})$ is increasing in ϕ'_{se} (note that $a \geq b$). Point (i) holds because $c(s,g,v,\phi_{se},r)$ is separately linear in ϕ_{se} and convex in r. Point (ii) holds because $J(s,g,v,\phi_{se})$ is increasing difference in (v,ϕ_{se}) according to the following Lemma 6. Based on point (i) and point (ii), and further based on the property that positive weighted sum keeps submodularity, we finish the proof that $Q(s,g,v,\phi_{se},r)$ is submodular in (ϕ_{se},r). Therefore, according to the property of submodularity [35] [23], the optimal rate allocation $r^*(1,g,v,\phi_{se}) = \arg\min_r Q(1,g,v,\phi_{se},r)$ is nondecreasing in ϕ_{se}. The proof with respect to ϕ_{id} follows the same method. □

Lemma 6: $J(s,g,v,\phi_{se})$ is increasing difference in (v,ϕ_{se}).

Proof of Lemma 6: Let $v_a \geq v_b$ denote two remaining payloads. Let $\phi_{se,1} \geq \phi_{se,2}$ denote two different levels of sensing power. To show that $J(s,g,v,\phi_{se})$ is increasing difference in (v,ϕ_{se}), it is equivalent to show

$$J(s,g,v_a,\phi_{se,1}) - J(s,g,v_b,\phi_{se,1}) \geq J(s,g,v_a,\phi_{se,2}) - J(s,g,v_b,\phi_{se,2}). \quad (35)$$

Let $J(s,g,v_a,\phi_{se,1}) = Q(s,g,v_a,\phi_{se,1},r_{a1})$ (i.e., $r_{a1} = \arg\min_z Q(s,g,v_a,\phi_{se,1},z)$). Similar definitions also apply to r_{a2}, r_{b1} and r_{b2}. By using the these definitions, condition (35) can be transformed into

$$\big(Q(s,g,v_a,\phi_{se,1},r_{a1}) - Q(s,g,v_b,\phi_{se,1},r_{b1})\big) - \big(Q(s,g,v_a,\phi_{se,2},r_{a2}) - Q(s,g,v_b,\phi_{se,2},r_{b2})\big) \geq 0.$$

Further manipulations on the above condition result in the following equivalent condition

$$Q(s,g,v_a,\phi_{se,1},r_{a1}) - Q(s,g,v_b,\phi_{se,1},r_{b2}) -Q(s,g,v_a,\phi_{se,2},r_{a1}) + Q(s,g,v_b,\phi_{se,2},r_{b2}) + A + B \geq 0,$$

where according to the definitions of $r_{a1}, r_{a2}, r_{b1}, r_{b2}$ given above, we have $A = Q(s,g,v_b,\phi_{se,1},r_{b2}) - Q(s,g,v_b,\phi_{se,1},r_{b1}) \geq 0$ and $B = Q(s,g,v_a,\phi_{se,2},r_{a1}) - Q(s,g,v_a,\phi_{se,2},r_{a2}) \geq 0$. Therefore, to prove (35), it is sufficient to show

$$Q(s,g,v_a,\phi_{se,1},r_{a1}) - Q(s,g,v_a,\phi_{se,2},r_{a1}) \geq Q(s,g,v_b,\phi_{se,1},r_{b2}) - Q(s,g,v_b,\phi_{se,2},r_{b2}) \geq 0,$$

which always holds by the definitions of Q-factor given in (7) and (8). □

[16]Note that when $s = 0$, the only feasible action is $a = b = 0$. Thus, our following proof is applicable when $s = 1$. This is consistent with our objective to prove that $r^*(1,g,v,\phi_{se})$ is nondecreasing in ϕ_{se}.

APPENDIX: PROOF OF EQUATION (14)

Proof of Equation (14): Based on condition (13), the solution $\hat{q}$ for problem (Stage-II) is a function of r_k, i.e., in the form of $\hat{q}(r_k)$. We first differentiate (13) with respect to r_k and obtain $\frac{d}{dr_k}\frac{V_k - r_k t_{tr}}{q(r_k)t_{tr}} = 0$. This result is equivalent to $(r_k - \frac{V_k}{t_{tr}})\frac{dq(r_k)}{dr_k} = q(r_k)$. Note that since $r_k - \frac{V_k}{t_{tr}}$ is nonpositive, $\frac{dq(r_k)}{dr_k}$ also has to be nonpositive. In other words, the optimal transmission duration $q(r_k)$ for the SU to finish its remaining payload $V_k - r_k t_{tr}$ is decreasing in the rate allocation r_k at the current slot k. This result is consistent with the intuitions. Moreover, this aforementioned differential equation indicates the solution that $\hat{q}(r_k) = (\frac{V_k}{t_{tr}} - r_k)C$. By setting $r_k = 0$ and putting $\hat{q}(r_k)$ back to (13), we obtain the condition for parameter C given by (15). Let function $M(\epsilon) = 2^\epsilon - 1 - (\ln 2)2^\epsilon\epsilon$. It can be shown that $\frac{dM(\epsilon)}{d\epsilon} = -2^\epsilon\epsilon(\ln 2)^2 < 0$. By further substituting $\epsilon = \frac{1}{C}$, we obtain function $L(C) = 2^{\frac{1}{C}} - 1 - (\ln 2)2^{\frac{1}{C}}\frac{1}{C}$, which is increasing in C. Furthermore, it can be verified that $\lim_{C\downarrow 0} L(C) = -\infty$ and $\lim_{C\uparrow\infty} L(C) = 0$. □

APPENDIX: PROOF OF LEMMA 2 AND LEMMA 3

Proof: The average number of slots for the SU to finish its target payload $V^{\max}$ can be approximated by $\frac{V}{\sum_{g\in\mathcal{G}}\sum_{v\in\mathcal{V}}\hat{r}(g,v)\Pr\{(g,v)\}}\frac{1}{\Theta_1}$, where $\Pr\{(g,v)\}$ represents the joint distribution of the event $(G_k = g, V_k = v)$. We aggressively ignore the constraint that $r_k \leq \frac{V_k}{t_{tr}}$, and the corresponding result corresponds to a lower bound for the average number of slots to finish $V^{\max}$. Meanwhile, by doing so, we obtain $\Pr\{(g,v)\} = \eta_g$, and the consequent low bound for the average delay can be given by (20). The approximation error in (20) stems from the situation that the remaining payload V_k is small, and the low-complexity rate allocation $\hat{r}_k$ is restricted by V_k strictly. Therefore, the lower bound (20) is asymptotically tight as $V^{\max} \to \infty$ and the impact from the limited V_k becomes more and more negligible. The approximated energy consumption (21) in Lemma 3 directly follows by the average number of slots to finish $V^{\max}$ given by (20). □

REFERENCES

[1] H. Kim, G. de Veciana, "Leveraging Dynamic Spare Capacity in Wireless Systems to Conserve Mobile Terminal's Energy," *IEEE Transactions on Networking*, vol. 18, no.3, pp. 802-815, June 2010

[2] E. Shih, P. Bahl, M.J. Sinclair, "Wake on Wireless: an Even Driven Energy Saving Strategy for Battery Operated Devices," in *Proc. of ACM MobiCom'2002*

[3] Y. Agarwal, R. Chandra, A Wolman, P. Bahl, K. Chin and R. Gupta, "Wireless Wakeups Revisited: Energy Management for VoIP over Wi-Fi Smartphones," in *Proc. of ACM MobiSys'2007*

[4] Sequans Communications, "Datasheet: SQN1130 System-on-Ship (SoC) for WiMax Mobile Stations"

[5] Atheros Communications, "AR5213 Preliminary Datasheet"

[6] G.K.W. Wong, Q. Zhang, D.H.K. Tsang, "Switching Cost Minimization in the IEEE 802.16e Mobile WiMAX Sleep Mode Operation", *Wireless Communications & Mobile Computing*, vol. 10, no. 2, pp. 1576-1588, Dec. 2010

[7] Y. Liang, Y. Zeng, E. Peh, A. Hoang, "Sensing-Throughput Tradeoff for Cognitive Radio Networks," *IEEE Transactions on Wireless Communications*, vol. 7, no. 4, pp. 1326-1337, April 2008

[8] H. Su, X. Zhang, "Energy-Efficient Spectrum Sensing for Cognitive Radio Networks," in Proc. of *IEEE ICC'2010*

[9] H. Kim, K.G. Shin, "Efficient Discovery of Spectrum Opportunities with MAC-Layer Sensing in Cognitive Radio Networks" *IEEE Transactions on Mobile Computing*, vol. 7, no. 5, pp. 533 - 545, May 2008

[10] R. Fan, H. Jiang,"Optimal Multi-Channel Cooperative Sensing in Cognitive Radio Networks," *IEEE Transactions on Wireless Communications*, vol. 9, no. 3, pp. 1128-1138, Mar. 2010.

[11] T.Y. Zhang, Y. Wu, K. Lang, D. H.K. Tsang, "Optimal Scheduling of Cooperative Spectrum Sensing in Cognitive Radio Networks", *IEEE System Journal*, vol. 4, no. 4, pp. 535-549, Dec. 2010

[12] N. B. Chang, M. Liu, "Optimal Channel Probing and Transmission Scheduling for Opportunistic Spectrum Access," *IEEE Trans. on Networking*, vol. 17, no. 6, pp. 1805-1818, December 2009

[13] Y. Chen, Q. Zhao, and A. Swami, "Distributed Spectrum Sensing and Access in Cognitive Radio Networks with Energy Constraint," *IEEE Transactions on Signal Processing*, vol. 57, no. 2, pp. 783-797, Feb. 2009

[14] A. Hoang, Y. Liang, D. Wong, Y. Zeng, and R. Zhang, "Opportunistic Spectrum Access for Energy-Constrained Cognitive Radios," *IEEE Transactions on Wireless Communications*, vol. 8, no. 3, pp. 1206-1211, Mar. 2009

[15] P. Venkatraman, B. Hamdaoui, M. Guizani, "Opportunistic Bandwidth Sharing Through Reinforcement Learning," *IEEE Transactions on Vehicular Technology*, vol. 59, no. 6, July 2010

[16] L. Zhang, Y. Xin, Y.C. Liang, H.V. Poor, "Cognitive Multiple Access Channels: Optimal Power Allocation for Weighted Sum Rate Maximization," *IEEE Transactions on Communications*, vol. 57, no. 9, pp. 2754-2762, Sept. 2009

[17] L. Gao, S. Cui, "Power and Rate Control in Cognitive Radio Networks via Dynamic Programming," *IEEE Transactions on Vehicular Technology*, vol. 58, no. 9, pp. 4819-4827, Nov. 2009

[18] H.A.B. Salameh, M. Krunz, O. Younis, "Cooperative Adaptive Spectrum Sharing in Cognitive Radio Networks," *IEEE/ACM Transactions on Networking*, vol. 18, no. 4, pp. 1181-1194, Aug. 2010

[19] J.W. Huang, V. Krishnamurthy, "Transmission Control in Cognitive Radio as a Markovian Dynmaic Game: Structural Result on Randomized Threshold Policies," *IEEE Transaction on Communications*, vol. 58, no. 1, Jan. 2010

[20] J. Zhu, J. Wang, T. Luo, S. Li, "Adaptive Transmission Scheduling over Fading Channels for Energy-Efficient Cognitive Radio Networks by Reinforcement Learning," *Telecommunication Systems*, vol. 42, pp. 123-138, 2009

[21] J. Lee, and N. Jindal, "Energy-efficient Scheduling of Delay Constrained Traffic over Fading Channels," *IEEE Transactions on Wireless Communiocations*, vol. 8, no. 4, pp. 1866-1875, April 2009

[22] A.K. Karmokar, D.V. Djonin, and V.K. Bhargava, "Optimal and Suboptimal Packet Scheduling over Correlated Time Varying Flat Fading Channels," *IEEE Transactions on Wireless Communications*, vol. 5, no. 2, pp. 446-456, Feb. 2006

[23] M.H. Ngo, V. Krishnmurthy, "Monotonicity of Constrained Optimal Transmission Policies in Correlated Fading Channels with ARQ," *IEEE Transactions on Signal Processing*, vol. 58, no. 1, pp. 438-451, Jan. 2010

[24] D.V. Djonin, V. Krishnmurthy, "Q-Learning Algorithms for Constrained Markov Decision Processes with Randomized Monotone Policies: Application to MIMO Transmission Control," *IEEE Transactions on Signal Processing*, vol. 55, no. 5, pp. 2170-2181 May 2007

[25] M. Morelli, M. Moretti, "Channel Estimation in OFDM Systems with Unknown Interference," *IEEE Transactions on Wireless Communications*, vol. 8, no. 8, pp. 5338-5347, Oct. 2009

[26] H.S. Wang, N. Moayeri, "Finite-state Markov model - a Useful Model for Radio Communication Channels," *IEEE Transactions on Vehicular Technology*, vol. 44, no. 1, pp. 163-171, Feb. 1995

[27] H.S. Wang, P.C. Chang, "On Verifying the First-Order Markovian Assumption for a Rayleigh Fading Channel Model," *IEEE Transactions on Vehicular Technology*, vol. 45, no. 2, pp. 353-357, May 1996

[28] Q. Zhang, S.A. Kassam, "Finite-state Markov model for Rayleigh fading channels," IEEE Transactions on Communications, vol. 47, no. 11, pp. 1688-1692, Nov. 1999

[29] F. Babich, G. Lombardi,"A Markov Model for the Mobile Propagation Channel," IEEE Transactions on Vehicular Technology, vol. 49, no. 1, pp. 63-73, Jan. 2000

[30] G. Yuan, R. Grammenos, Y. Yuan, W. Wang, "Performance Analysis of Selective Opportunisitic Spectrum Access With Traffic Prediction," *IEEE Transaction on Vehicular Technology*, vol. 59, no. 4, May 2010

[31] F.J. Beutler, K.W. Ross, "Optimal Policies for Controlled Markov Chain with a Constraint," *Journal of Mathematical Analysis and Applications*, vol. 112, pp. 236-252, 1985

[32] Cisco Inc, "Voice over IP - Per Call Bandwidth Consumption"

[33] IEEE802.22 Wireless RAN, "Functional Requirements for the 802.22RAN Standard," IEEE Std. 802.22-05/00007r46,
[34] S.M. Ross, *Introduction to Probability Models*, 8th ed. Academic Press, 2003
[35] D.M. Topkis, *Supermodularity and complementarity*, Princeton University Press, 1998
[36] D.P. Bersekas, *Dynamic Programming and Optimal Control*, 3rd ed., Athena Scientific, 2005, vol. 1
[37] G.L. Stuber, *Principles of Mobile Communication*, Kluwer Academic, 1996